

High energy neutrinos from the Sun

Manuel Masip

*CAFPE and Departamento de Física Teórica y del Cosmos
Universidad de Granada, E-18071 Granada, Spain*

`masip@ugr.es`

Abstract

The Sun is a main source of high energy neutrinos. These neutrinos appear as secondary particles after the Sun absorbs high-energy cosmic rays, that find there a low-density environment (much thinner than our atmosphere) where most secondary pions, kaons and muons can decay before they lose energy. The main uncertainty in a calculation of the solar neutrino flux is due to the effects of the magnetic fields on the absorption rate of charged cosmic rays. We use recent data from HAWC on the cosmic-ray shadow of the Sun to estimate this rate. We evaluate the solar neutrino flux and show that at 1 TeV it is over ten times larger than the atmospheric one at zenith $\theta_z = 30^\circ/150^\circ$. The flux that we obtain has a distinct spectrum and flavor composition: it is harder and richer in antineutrinos and tau/electron neutrinos than the atmospheric background. This solar flux could be detected in current and upcoming neutrino telescopes. KM3NeT, in particular, looks very promising: it will see the Sun high in the sky (the atmospheric flux is lower there than near the horizon) and expects a very good angular resolution (the Sun's radius is just 0.27°).

1 Introduction

High-energy astroparticles provide a picture of the sky that complements the traditional one from light in different frequencies. They reach the Earth with a spectrum that extends up to 10^{11} GeV, millions of times above the energies that we are able to achieve at particle colliders. Their study for over 100 years has defined a puzzle that, although not complete yet, has helped us to understand the environment where these particles are produced: supernovas, pulsars, active galactic nuclei or gamma ray bursts, where nature reaches its most extreme conditions.

Neutrinos are an essential piece in that puzzle. They appear whenever a cosmic proton or a heavier nucleus interacts with matter or light and fragments into secondary neutrons, pions and kaons, which decay giving leptons. In astronomy neutrinos are a *unique* messenger: unlike charged cosmic rays (CRs), they are not deflected by magnetic fields and point to the source; unlike gamma rays, they can propagate through a dense medium and reach the Earth unscattered. Their promise, however, faces two main challenges. First, being weakly-interacting particles, they are very difficult to detect: neutrino telescopes require large volumes in order to register just a few events. In addition, neutrinos are constantly produced when high-energy cosmic rays enter the atmosphere and start an air shower. Any astrophysical signal must then be separated from this atmospheric background. Despite that, the recent discovery by IceCube [1] of a diffuse flux of cosmic origin proves that high-energy neutrino astronomy is indeed possible.

Here we will discuss an astrophysical flux that has a precise location in the sky and a known spectrum and composition: the high-energy neutrino flux from our Sun. Proposed in the early 90's [2, 3], this flux has recently attracted renewed attention [4–6]. Its interest is threefold. First of all, the solar flux is well above the atmospheric background. If detected and characterized, it could be used to calibrate the energy and the angular resolution of neutrino telescopes. KM3Net [7], in particular, will be able to follow the Sun at relatively vertical directions ($\theta_z \geq 135^\circ$ or $\theta_z \leq 45^\circ$): the high-energy atmospheric background is much smaller there than from the near-horizontal directions typical at IceCube. In addition, the analysis of this neutrino flux would certainly bring valuable information about the solar magnetic field [2]. Finally, as emphasized in the most recent work [4–6], this flux is itself a strong background in the search for dark matter annihilation in the Sun [8–11].

Our calculation will differ from previous ones in some significant aspects. The results at $E < 1$ TeV depend crucially on the magnetic fields present in the inner solar system [2]. In the next section we argue that HAWC data [12] on the cosmic ray shadow of the Sun can be of use for an estimate. In our analysis we pay special attention to the yields in hadron

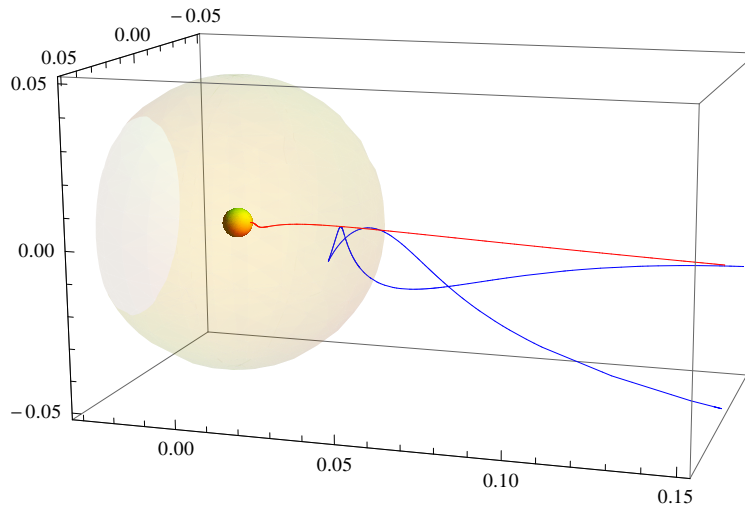


Figure 1: Trajectories through the Parker field with origin at the Earth for 1 TeV (reflected) and 5 TeV (absorbed) protons. We have shaded the region $R < 10R_{\odot}$ (in AU).

collisions: we use EPOS-LHC [13] to deduce the (energy dependent) yields $f_{hh'}(x, E)$ of all the long-lived species ($p, n, \bar{p}, \bar{n}, \pi^{\pm}, K^{\pm}, K_L$). In addition, in pion and kaon decays we will distinguish the production of positive and negative helicity muons, which imply very different neutrino yields. Finally, our solar model takes into account the ionization of the hydrogen and helium in the interior of the Sun, implying a lower rate of energy loss as muons propagate.

2 Magnetic effects on cosmic rays

The magnetic effects of the Sun on CRs may be separated into three basic regions.

(i) At distances $R \geq 10R_{\odot}$ [14] and $E \geq 100$ GeV the Parker (interplanetary) field [15] will basically define ballistic trajectories. Many of these trajectories will be magnetically mirrored before getting to that limit (see Fig. 1), but CRs can always find a ballistic trajectory close to a field line that connects the Earth with the region $R \approx 10R_{\odot}$.

(ii) At $R < 10R_{\odot}$ the field lines tend to co rotate with the Sun; magnetic fluctuations become dominant and the field intensity is very dependent on the phase in the solar cycle. In the corona, at midlatitudes and the equator most field lines are closed into loops that start and finish in the solar surface, whereas the interplanetary field lines are pushed to the polar regions. Above the solar transition region (between the chromosphere and the corona) the propagation of $E \leq 1$ TeV CRs is probably best described by a diffusion equation. In particular, an energy-dependent diffusion coefficient that decreases as CRs approach the Sun's surface would favor their *reflection* by the increasing magnetic field strength that they

face.

(iii) In the chromosphere and the photosphere it is gas pressure and fluid dynamics (instead of the magnetic field) what dictates the solar structure. One could use geometric arguments and individual CR trajectories to estimate the absorption rate and, most remarkably, to study the possibility of an *albedo* flux: the flux of cascade products reflected from the surface [2] (see also [16] for a discussion of the gamma-ray flux from the solar disk).

We can use data on the CR shadow of the Sun, which was first seen by TIBET [17] and then by other observatories, to justify and quantify these magnetic effects. The solar field acts on CRs as a magnetic lens, and we know from Liouville theorem that its only possible effect on the primary flux is to create a shadow: a lens (including a mirror) will not make anisotropic an isotropic flux, but it may interrupt (absorb) trajectories that were aiming to the Earth. Therefore, the presence of a shadow reveals the absorption of CRs by the Sun.

Let us focus on the data taken by HAWC [12] during the years 2013-2014, near a solar maximum. HAWC detected the shadow already at $E \approx 2$ TeV. It is not a black disk (a 100% CR deficit) of 0.27° radius (the angular radius of the Sun); instead, the shadow is a deficit that decreases radially as we move away from the angular position of the Sun:

$$d(\theta) \approx -A \exp\left(-\frac{\theta^2}{2\sigma^2}\right), \quad (1)$$

being A and σ energy-dependent parameters. At $E \approx 8$ TeV HAWC finds $A = 0.005$ and $\sigma = 1.4^\circ$; the shadow is *diluted* both by the experimental error and by the solar magnetic field into an angular area that corresponds quite closely to the $R < 10R_\odot$ region that we assumed dominated by magnetic turbulence. Moreover, integrating to find the total CR deficit we obtain that it represents a 27% of the full shadow of the Sun, $D_\odot = -\pi (0.27^\circ)^2$. This indicates that the Sun absorbs just 27% of the 8 TeV CRs that were headed towards the Earth, while the remaining 73% were deflected (mirrored) and reached us.

At higher energies, $E \approx 50$ TeV, their fit gives $A = 0.013$ and $\sigma = 1.7^\circ$. The shadow is again diffused into an angular region ten times larger than the actual size of the Sun, but now we see the whole total deficit, with no reflexion:

$$D_\odot^{-1} \int d\theta 2\pi\theta d(\theta) \approx 1. \quad (2)$$

At these energies there is a full set of CR trajectories that were aiming to the Earth through the solar magnetic field and were interrupted (absorbed) by the Sun. In contrast, at $E \approx 2$ TeV ($A = 0.0013$ and $\sigma = 1.2^\circ$) the observed deficit amounts to just 6% of the Sun's shadow, implying that up to 94% of CRs were unable to reach the surface.

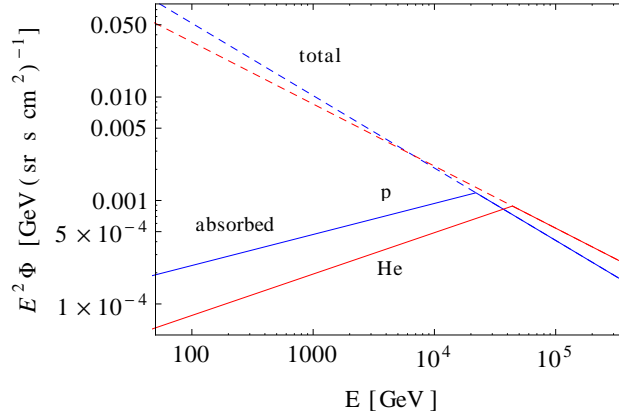


Figure 2: Total and absorbed CR fluxes (see text).

The previous analysis motivates the following fluxes (in Fig. 2). At $E < E_{\text{knee}}^*$ we take [18] a two-component primary flux with proton and He nuclei [in particles/(GeV sr s cm²)]:

$$\Phi_p = 1.3 \left(\frac{E}{\text{GeV}} \right)^{-2.7} \quad \Phi_{\text{He}} = 0.54 \left(\frac{E}{\text{GeV}} \right)^{-2.6} \quad (3)$$

At $E > 22$ TeV for proton and $E > 44$ TeV for helium (*i.e.* at CR rigidities $R > 22$ TV) the absorbed and the total fluxes coincide. At lower energies, however, the spectral index of the absorbed fluxes changes to -1.7 and -1.6 for proton and He, respectively. This change reproduces the deficits that we have discussed above. Since the HAWC data corresponds to a solar maximum, we will also consider an absorbed flux where the spectral change occurs at lower energies, $R = 22/3$ TV, as a possibility for a quiet Sun.

3 Solar showers

In order to understand the solar flux it may be useful to review the sequence of events taking place after a high-energy CR enters the Earth's atmosphere [19]. Consider a primary proton of $E > 100$ GeV, energies where we can neglect the effects of the Earth's magnetosphere. Its first interaction with an air nucleus will typically occur at 20 km of altitude, after it has crossed a hadronic interaction length (*e.g.*, $\lambda_p^{\text{int}} = 70$ g/cm² at $E = 10^5$ GeV). As a result, the proton will fragment into a *leading baryon* carrying 35% of the initial energy plus dozens of secondary hadrons, mostly mesons. The leading baryon will interact again deeper into the atmosphere, but after just four collisions 99% of its energy will already be deposited in the air. Secondary charged pions and kaons, in turn, may collide giving more mesons of lower

*We have assumed that the proton (He) spectrum changes to a $E^{-3.0}$ power law at $10^{6.3}$ ($10^{6.5}$) GeV.

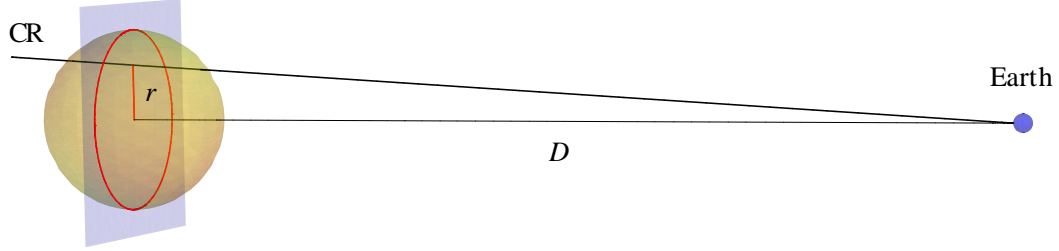


Figure 3: The CR enters the Sun at a transverse distance $r \leq R_\odot$, producing neutrinos that will reach the Earth at an angular distance $r/D \leq 0.27^\circ$ from the Sun's center.

energy or they may decay giving leptons, *e.g.*, $\pi^+ \rightarrow \mu^+ \nu_\mu$. The probability that they do one thing or the other depends on their energy and on the air density that they find. For example, a 10 GeV π^+ is more likely to decay than collide, since its (Lorentz dilated) 560 m decay length is shorter than the typical interaction length in the upper atmosphere. At 100 GeV, however, the pion will probably hit an air nucleus before it has completed its 5.6 km decay length. Since the higher the energy the less likely they are to decay, the atmospheric neutrino flux from parent pions and kaons is very suppressed at high energies, specially from vertical directions (from larger zenith angles they face a thinner atmosphere at the same slant depth). Notice also that most muons of energy above 5 GeV will hit the ground and lose there the energy before they decay and give neutrinos, $\mu^+ \rightarrow e^+ \nu_e \bar{\nu}_\mu$.

It is easy to realize that the sequence will be quite different if the same primary proton hits the Sun's surface. Let us discuss these differences in some detail.

(i) First of all it will find a medium that is much thinner than our atmosphere. The photosphere, extending up to 500 km above the Sun's optical surface, has a density between 3×10^{-9} and 2×10^{-7} g/cm³ (we will use the solar model in [20]). A CR that crosses it vertically will face a total depth (column density) of just 2.7 g/cm², whereas if the CR enters from a radial parameter $r = 0.9R_\odot$ (see Fig. 3) the total depth of the photosphere increases to 6.2 g/cm². Moreover, when the CR goes deeper it will not find a sharp change in the Sun's density. For example, it takes 1500 km to cross 100 g/cm² from $r = 0$ or up to 2600 km from $r = 0.9$. The decay length of a 10 TeV charged pion is 557 km, so most mesons produced there will have plenty of time to decay and give high-energy neutrinos.

(ii) The hadronic shower will then develop within the initial 2000 km inside the Sun,

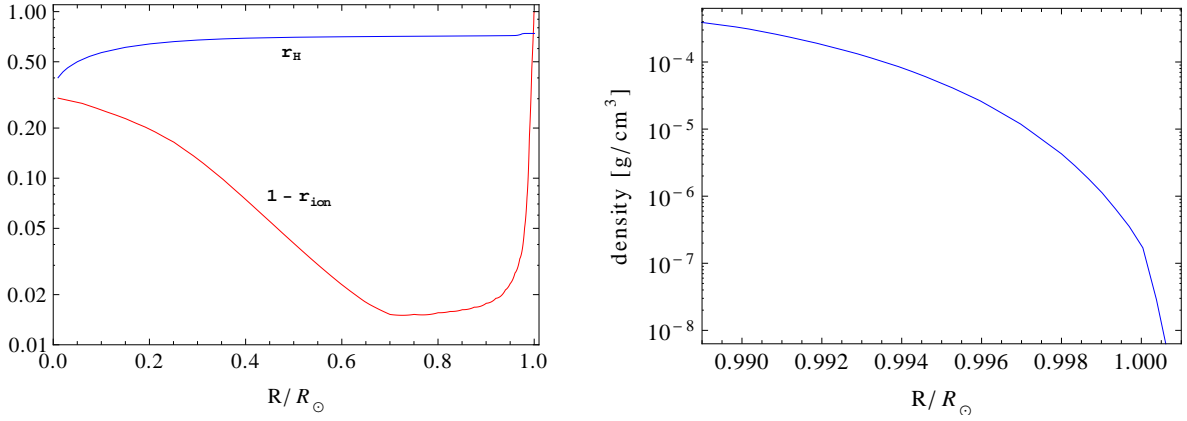


Figure 4: Fraction of hydrogen (r_H) and of ionized matter (r_{ion}) at different radii inside the Sun and mass density near the surface.

where the mass density (74% hydrogen and the rest mostly ^4He [21]) is always below 10^{-5} g/cm 3 (see Fig. 4). We have used EPOS-LHC [13] to parametrize the hadronic cross sections for nucleon, pion and kaon collisions as well as the yields $f_{hh'}(x, E)$ of secondary hadrons ($h' = p, n, \bar{p}, \bar{n}, \pi^\pm, K^\pm, K_L$) carrying a fraction x of the incident energy E after these collisions. In particular, we have simulated 50,000 collisions for each primary and for several energies; we have then deduced the yields at those energies and have used an interpolation to obtain $f_{hh'}(x, E)$ in the whole 10 – 10^8 GeV interval. To illustrate our results, in Fig. 5 we plot the yields in $E = 10^5$ GeV p and π^+ collisions with a proton at rest.

(iii) After a few thousand km all the hadrons in the shower have been absorbed or have decayed, and only the neutrino and high-energy muon components survive. The muons will then propagate along the thin medium near the Sun's surface, so they will have a significant probability to decay when their energy is still high. For example, it would take 1.8×10^4 km if $r = 0$ or 3.4×10^4 km if $r = 0.9R_\odot$ to cross a total depth of just 15 km w.e. There are two important factors that change the muon propagation there relative to the one we observe at the Earth [22]. First, at high energies energy loss through radiative processes will be caused by the low- Z nuclei in the Sun, and second, these nuclei are partially ionized, resulting into a reduced rate of muon energy loss also at lower energies. We estimate a mean energy loss per unit depth t

$$-\frac{d\langle E_\mu \rangle}{dt} = (1 - r_{\text{ion}}) \left[r_H (a^H - a^{\text{He}}) + a^{\text{He}} \right] + \left[r_H (b^H - b^{\text{He}}) + b^{\text{He}} \right] E_\mu, \quad (4)$$

where r_{ion} is the fraction of ionized matter deduced from Saha equation (it goes from 10^{-4} near the Sun's surface to 0.96 at a depth of 15 km w.e., see Fig. 4), r_H is the hydrogen fraction, $a^H = 4.8$ MeV cm 2 /g, $a^{\text{He}} = 2.8$ MeV cm 2 /g, $b^H = 2.1 \times 10^{-6}$ cm 2 /g, and $b^{\text{He}} = 1.6 \times 10^{-6}$

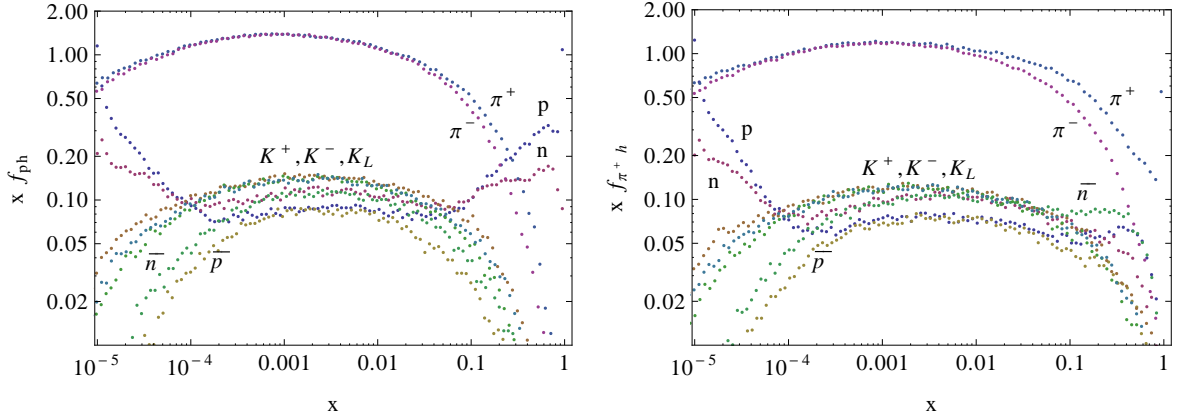


Figure 5: Yields in pp (left) and π^+p (right) collisions at $E = 10^5$ GeV.

cm^2/g . Notice that the higher rate of muon decays in the Sun relative to terrestrial air showers will induce a substantially different $\nu_e:\nu_\mu$ ratio at $E > 10$ GeV.

(iv) After a depth of 15 km w.e. most muons have already decayed and we are left with only neutrinos. These neutrinos, however, still have to cross a large fraction of the Sun's volume before they can emerge from the opposite side and reach the Earth (see Fig. 3). Their absorption will introduce a significant suppression of higher energies in this ν flux, specially for low values of r . The absorption length λ_ν for a 100 GeV neutrino is around 7.9×10^{12} g/cm^2 [23]; since the total depth of the Sun goes from 3.0×10^{12} g/cm^2 at $r = 0$ to 8.7×10^8 g/cm^2 at $r = 0.9R_\odot$, most of these neutrinos will not be absorbed. At $E_\nu = 1$ TeV λ_ν is reduced to 2.8×10^{11} g/cm^2 , which is longer than the solar depth only for $r \geq 0.33R_\odot$. At these energies the antineutrinos have a 3 times longer absorption length, which favors them *versus* neutrinos. At $E_\nu = 100$ TeV we have $\lambda_\nu = 7.6 \times 10^9$ g/cm^2 , and only the neutrinos crossing the Sun at $r \geq 0.74R_\odot$ will more likely emerge than being absorbed.

(v) A final but important effect are the flavor oscillations [24]. As shown in [25], matter effects are suppressed when averaged over the production region and over the ν and $\bar{\nu}$ components, and the final flavor is dominated by oscillations in vacuum between the Sun and the Earth. In particular, muon and electron neutrinos will experience multiple oscillations into the ν_τ flavor at energies $E < 70$ TeV and $E < 2$ TeV, respectively.

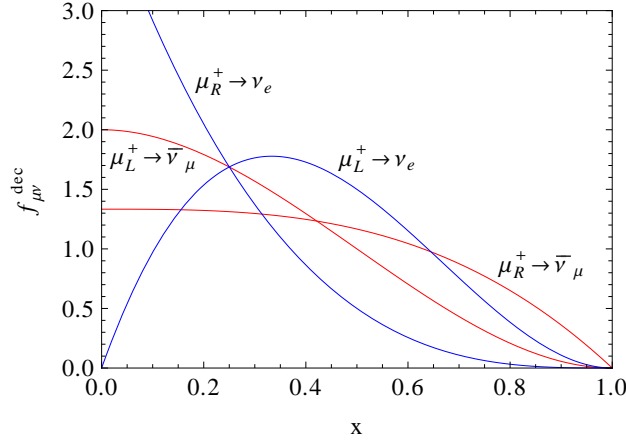


Figure 6: Yields of muon and electron neutrinos in the decay of positive (μ_R) and negative (μ_L) helicity muons.

4 Neutrino fluxes

As discussed in Section 2, the CRs that we do *not* see at the Earth have showered near the Sun's surface. We have also learned in the previous section that secondaries of up to several TeV will have plenty of time to decay there before they collide and lose energy. In contrast with what happens in the Earth atmosphere, this will be the case for showers entering the Sun from any zenith angle, and independent of how *curly* the trajectory of secondary pions, kaons and muons becomes. We will then assume that the Sun emission is near isotropic. In addition, at $E < 1$ TeV the absorption of neutrinos by the Sun will not be significant. This means that at these neutrino energies any CR trajectory is equally good to determine the ν flux emitted by the Sun: we will take a straight shower entering from the opposite side of the Sun like the one in Fig. 3. Notice that the albedo flux of neutrinos in that side of the Sun will be compensated by a similar albedo flux in the side facing the Earth.

At higher energies ($E \geq 1$ TeV) the neutrino absorption by the Sun will be important. The pions producing these neutrinos, however, are very energetic and their trajectory will be less affected by the solar magnetic fields. Therefore, we think that the straight showers entering the Sun with parameter r between 0 and R_\odot (see Fig. 3) may provide a good approximation for the flux at all neutrino energies.

It is then easy to deduce the transport equations for the 9 long-lived hadron species ($h = p, n, \bar{p}, \bar{n}, \pi^\pm, K^\pm, K_L$), muons of left and right-handed helicity ($\mu = \mu_L^\pm, \mu_R^\pm$) and neutrinos ($\nu = \nu_{e,\mu}, \bar{\nu}_{e,\mu}$). It is necessary to distinguish between both muon helicities, as their decay (in Fig. 6) implies very different neutrino distributions [26] (see also [27] for the lepton yields

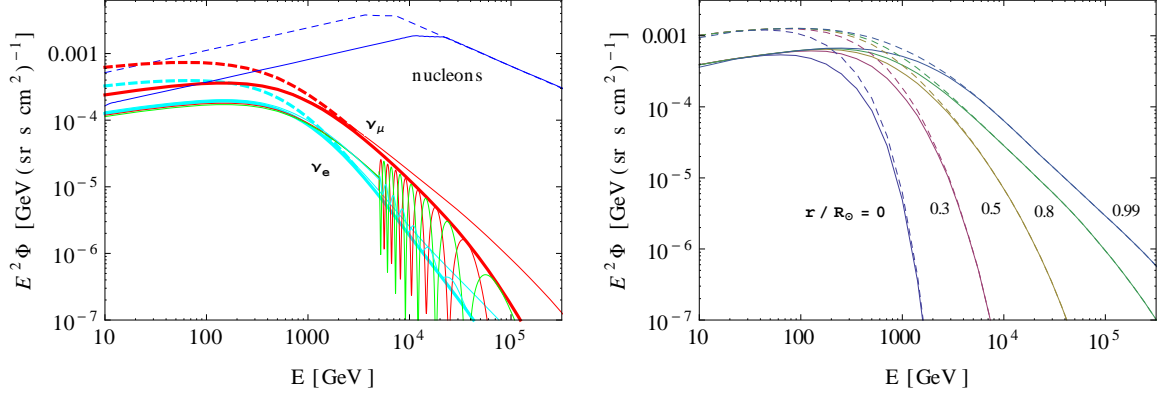


Figure 7: **Left:** $\nu+\bar{\nu}$ and primary nucleon fluxes for $r = 2/3 R_{\odot}$. Red, cyan and green lines correspond to the ν_{μ} , ν_e and ν_{τ} fluxes, respectively. They are given at 15 km w.e. (upper thin lines), after the partial absorption by the Sun (thick lines), and at the Earth (lower thin lines). Below 5 TeV we plot the averaged oscillations (the lines for the three flavors almost coincide). **Right:** Total flux at the Earth for different values of r . Solid and dashed lines correspond to our modelization of the absorption rate for maximum and minimum of Solar activity, respectively.

from 3-body meson decays). The generic equations are

$$\begin{aligned} \frac{d\Phi_i(E, t)}{dt} = & -\frac{\Phi_i(E, t)}{\lambda_i^{\text{int}}(E, t)} - \frac{\Phi_i(E, t)}{\lambda_i^{\text{dec}}(E, t)} + \sum_{j=h} \int_0^1 dx \frac{f_{ji}(x, E/x)}{x} \frac{\Phi_j(E/x, t)}{\lambda_j^{\text{int}}(E/x, t)} + \\ & \sum_{k=h, \mu} \int_0^1 dx \frac{f_{ki}^{\text{dec}}(x, E/x)}{x} \frac{\Phi_k(E/x, t)}{\lambda_j^{\text{dec}}(E/x, t)}, \end{aligned} \quad (5)$$

where the sources include both collisions and decays and the interaction/decay lengths are expressed in g/cm^2 . The equations for the muon fluxes have the extra term

$$\frac{d\Phi_{\mu}(E, t)}{dt} \supset -\frac{d\langle E_{\mu} \rangle}{dt} \frac{d\Phi_{\mu}(E, t)}{dE} - \Phi_{\mu}(E, t) \frac{d}{dE_{\mu}} \left(\frac{d\langle E_{\mu} \rangle}{dt} \right), \quad (6)$$

describing energy loss. We do not include flavor oscillations in the transport of neutrinos inside the Sun. The numerical resolution of these 17 equations provides then the following results.

In Fig. 7–left we take $r = 2/3 R_{\odot}$, which is the average radial distance in a circle, and plot (i) the neutrino flux at a Solar depth of 15 km w.e. (thin red and cyan lines for ν_{μ} and ν_e , respectively), (ii) the flux after crossing the Sun (thick red and cyan lines), and (iii) the final ν flux at the Earth for the three neutrino flavors (thin cyan, red and green lines for ν_e ,

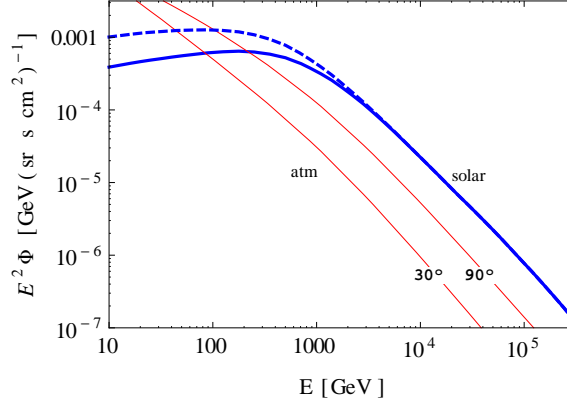


Figure 8: Comparison of the solar and the atmospheric (for two zenith angles) fluxes. The first one has been averaged over the whole solid angle occupied by the Sun (a circle of 0.27° radius). Solid and dashed lines correspond to our modelization of the absorption rate for maximum and minimum of Solar activity, respectively.

ν_μ and ν_τ , respectively). In the plot we include the primary all-nucleon flux (protons plus neutrons bound in helium) for the absorbed flux deduced from HAWC near a solar maximum (solid) and another one that could correspond to a quieter solar phase (dashes). We can see that ν oscillations play a crucial role: at $E \approx 70$ TeV most muon neutrinos have oscillated into the ν_τ flavor; at $E \leq 1$ TeV the three (averaged) flavors are almost undistinguishable, and they coincide with the ν_e flux before oscillations (thick cyan line). In our analysis we have taken the neutrino masses and mixings deduced in [28].

Fig. 7–right gives the total neutrino flux reaching the Earth from different radial distances r . As expected, at $E > 1$ TeV the flux from the center ($r = 0$) is much weaker than from the peripheral regions. Notice also that the lower-energy fluxes do not depend on r , indicating that the longitudinal development of the shower is independent of the zenith angle.

Finally, in Fig. 8 we compare the average solar flux with the atmospheric one [26] from two different zenith angles. At 500 GeV the solar flux (neutrinos plus antineutrinos of all flavors) is 7.0 (2.0) times larger than the atmospheric one from $\theta_z = 30^\circ/150^\circ$ ($\theta_z = 90^\circ$). At 5 TeV, the relative difference with the atmospheric flux increases: 20.5 times larger from $\theta_z = 30^\circ/150^\circ$ and 4.0 times larger from horizontal directions. If we restrict to the ν_μ flavor, at 5 TeV the average flux from the Sun is 7.0 and 1.4 times larger than the atmospheric one from those two inclinations, respectively. Notice that the atmospheric background is significantly stronger when the Sun is seen at large zenith angles.

Our calculation of the high-energy solar neutrino flux has several sources of uncertainty.

Different hadronic models imply lepton yields that typically differ in a 10% (see the comparison between EPOS-LHC and SIBYLL [29] in [30]). However, at $E_\nu > 1$ TeV the main uncertainty in our result comes from the 10–1000 TeV all-nucleon flux, whose accuracy may be estimated at 20% [18, 22]. At lower neutrino energies our calculation relies strongly on the absorption rate by the Sun of 0.1–10 TeV CRs, something that is given by HAWC with a $\approx 20\%$ uncertainty and that is expected to change during the solar cycle. The available data from HAWC corresponds to a solar maximum in 2013–2014, and thus the ≈ 100 GeV ν flux could increase substantially during the next years (a 50% in our estimate, see Fig. 8).

5 Summary and discussion

It seems quite plausible that the Sun is the most luminous object in the sky also for high energy neutrinos. We think that the existence of a known source that gives a signal above the atmospheric background can be useful for the development of neutrino telescopes. The atmospheric background is certainly stronger from the near horizontal directions that point to the Sun at IceCube than from the more vertical ones at KM3NeT, but features like the presence of a strong ν_τ component (which is absent in the atmospheric flux) offer hope that it can be observed also there.

We have correlated this high-energy neutrino signal with HAWC’s observations of a CR deficit from the Sun. Our results are qualitatively very similar to the ones in [2], but at high energies imply a neutrino flux slightly higher than the recent ones obtained in [4–6]. Indeed, a measurement of the Sun’s shadow during its whole 11-year cycle would imply a more precise prediction of this solar neutrino flux, specially at $E_\nu \leq 1$ TeV. Its detection and analysis at neutrino telescopes will improve our understanding of the magnetic properties and the internal structure of the Sun.

Acknowledgments

The author would like to thank Miquel Ardid, Eduardo Battaner, John Beacom, Joaquín Castellano, Joakim Edsjo, Juanjo Hernández, Kenny Ng, Aaron Vincent and Juande Zornoza for comments and discussions. This work has been supported by MICINN of Spain (FPA2013-47836, FPA2015-68783-REDT, FPA2016-78220, Consolider-Ingenio **MultiDark** CSD2009-00064) and by Junta de Andalucía (FQM101).

References

- [1] M. G. Aartsen *et al.* [IceCube Collaboration], *Science* **342** (2013) 1242856.
- [2] D. Seckel, T. Stanev and T. K. Gaisser, *Astrophys. J.* **382** (1991) 652.
- [3] I. V. Moskalenko, S. Karakula and W. Tkaczyk, *Astron. Astrophys.* **248** (1991) L5.
- [4] C. A. Argelles, G. de Wasseige, A. Fedynitch and B. J. P. Jones, “Solar Atmospheric Neutrinos and the Sensitivity Floor for Solar Dark Matter Annihilation Searches,” arXiv:1703.07798 [astro-ph.HE].
- [5] K. C. Y. Ng, J. F. Beacom, A. H. G. Peter and C. Rott, “Solar Atmospheric Neutrinos: A New Neutrino Floor for Dark Matter Searches,” arXiv:1703.10280 [astro-ph.HE].
- [6] J. Edsjo, J. Elefant, R. Enberg and C. Niblaeus, “Neutrinos from cosmic ray interactions in the Sun,” arXiv:1704.02892 [astro-ph.HE].
- [7] S. Adrián-Martínez *et al.* [KM3NeT Collaboration], *JHEP* **1705** (2017) 008
- [8] S. Adrian-Martinez *et al.* [ANTARES Collaboration], *JCAP* **1311** (2013) 032.
- [9] S. Adrian-Martinez *et al.* [ANTARES Collaboration], *Phys. Lett. B* **759** (2016) 69.
- [10] M. Ardid, I. Felis, A. Herrero and J. A. Martínez-Mora, *JCAP* **1704** (2017) no.04, 010.
- [11] M. G. Aartsen *et al.* [IceCube Collaboration], *Eur. Phys. J. C* **77** (2017) no.3, 146.
- [12] O. Enriquez-Rivera *et al.* [HAWC Collaboration], *PoS ICRC 2015* (2016) 099.
- [13] T. Pierog, I. Karpenko, J. M. Katzy, E. Yatsenko and K. Werner, *Phys. Rev. C* **92** (2015) 034906.
- [14] R. C. Tautz, A. Shalchi and A. Dosch, *J. Geophys. Res. Space Phys.* **116** (2011) 2102.
- [15] E. N. Parker, *Astrophys. J.* **128** (1958) 664.
- [16] B. Zhou, K. C. Y. Ng, J. F. Beacom and A. H. G. Peter, “TeV Solar Gamma Rays From Cosmic-Ray Interactions,” arXiv:1612.02420 [astro-ph.HE].
- [17] M. Amenemori *et al.* [TIBET AS γ Collaboration], *Astrophys. J.* **541** (2000) 1051.
- [18] M. Boezio and E. Mocchiutti, *Astropart. Phys.* **39-40** (2012) 95.
- [19] T. K. Gaisser, Cambridge, UK: Univ. Pr. (1990) 279 p

- [20] J. Christensen-Dalsgaard *et al.*, Science **272** (1996) 1286.
- [21] J. N. Bahcall and M. H. Pinsonneault, Phys. Rev. Lett. **92** (2004) 121301.
- [22] C. Patrignani *et al.* [Particle Data Group], Chin. Phys. C **40** (2016) no.10, 100001.
- [23] A. Connolly, R. S. Thorne and D. Waters, Phys. Rev. D **83** (2011) 113009.
- [24] C. Hettlage, K. Mannheim and J. G. Learned, Astropart. Phys. **13** (2000) 45.
- [25] G. L. Fogli, E. Lisi, A. Mirizzi, D. Montanino and P. D. Serpico, Phys. Rev. D **74** (2006) 093004.
- [26] P. Lipari, Astropart. Phys. **1** (1993) 195.
- [27] J. I. Illana, P. Lipari, M. Masip and D. Meloni, Astropart. Phys. **34** (2011) 663.
- [28] M. C. Gonzalez-Garcia, M. Maltoni and T. Schwetz, JHEP **1411** (2014) 052.
- [29] E. J. Ahn, R. Engel, T. K. Gaisser, P. Lipari and T. Stanev, Phys. Rev. D **80** (2009) 094003.
- [30] J. M. Carceller and M. Masip, JCAP **1703** (2017) 013.